Parathyroid Hormone Receptor Signaling Induces Bone Resorption in the Adult Skeleton by Directly Regulating the *RANKL* Gene in Osteocytes

Abdullah N. Ben-awadh, Jesus Delgado-Calle, Xiaolin Tu, Kali Kuhlenschmidt, Matthew R. Allen, Lilian I. Plotkin, and Teresita Bellido

Departments of Anatomy and Cell Biology (A.N.B., J.D.-C., X.T., K.K., M.R.A., L.I.P., T.B.) and Medicine (T.B.), Division of Endocrinology, Indiana University School of Medicine, and Roudebush Veterans Administration Medical Center (J.D.-C., L.I.P., T.B.), Indianapolis, Indiana 46202

PTH upregulates the expression of the receptor activator of nuclear factor κB ligand (*Rankl*) in cells of the osteoblastic lineage, but the precise differentiation stage of the PTH target cell responsible for RANKL-mediated stimulation of bone resorption remains undefined. We report that constitutive activation of PTH receptor signaling only in osteocytes in transgenic mice (DMP1-caPTHR1) was sufficient to increase *Rankl* expression and bone resorption. Resorption in DMP1-caPTHR1 mice crossed with mice lacking the distal control region regulated by PTH in the *Rankl* gene ($DCR^{-/-}$) was similar to DMP1-caPTHR1 mice at 1 month of age, but progressively declined to reach values undistinguishable from wild-type (WT) mice at 5 months of age. Moreover, DMP1-caPTHR1 mice exhibited low tissue material density and increased serum alkaline phosphatase activity at 5 month of age, and these indices of high remodeling were partially and totally corrected in compound DMP1-caPTHR1;$DCR^{-/-}$ male mice, and less affected in female mice. *Rankl* expression in bones from DMP1-caPTHR1 mice was elevated at both 1 and 5 months of age, whereas it was high, similar to DMP1-caPTHR1 mice at 1 month, but low, similar to WT levels at 5 months in compound mice. Moreover, PTH increased *Rankl* and decreased *Sost* and *Opg* expression in ex vivo bone organ cultures established from WT mice, but only regulated *Sost* and *Opg* expression in cultures from $DCR^{-/-}$ mice. PTH also increased *RANKL* expression in osteocyte-containing primary cultures of calvarial cells, in isolated murine osteocytes, and in WT but not in $DCR^{-/-}$ osteocyte-enriched bones. Thus, PTH upregulates *Rankl* expression in osteocytes in vitro, ex vivo and in vivo, and resorption induced by PTH receptor signaling in the adult skeleton requires direct regulation of the *Rankl* gene in osteocytes. **(*Endocrinology* 155: 2797–2809, 2014)**

Accumulating evidence demonstrates that some of the actions of PTH on the skeleton are mediated by direct effects of the hormone on osteocytes, the most abundant and highly communicated cells in bone (1). PTH downregulates the expression of the *Sost* gene, which encodes the potent inhibitor of bone formation sclerostin, expressed by osteocytes in bone (2, 3), and also increases the expression of fibroblast growth factor 23 (*Fgf23*), a hormone expressed in osteocytes (and osteoblasts) that regulates phosphate reabsorption in the kidney, contributing to mineral homeostasis (1, 4, 5).

Earlier studies have shown that the major skeletal effects of PTH are recapitulated in transgenic mice expressing a constitutively active PTH receptor in osteocytes, named DMP1-caPTHR1 mice (1, 4, 6, 7). Bones from these transgenic mice exhibit decreased *Sost*/sclerostin expression and elevated Wnt signaling, increased osteoblasts and bone formation, and a remarkable increase in bone mineral density (BMD) in both the axial and appendicular

ISSN Print 0013-7227 ISSN Online 1945-7170
Printed in U.S.A.

Received January 21, 2014. Accepted May 16, 2014.
First Published Online May 30, 2014

Abbreviations: BFR, bone formation rate; BMD, bone mineral density; CTX, C-telopeptide fragments of type I collagen; DBA, dibutyryl cAMP; DCR, distal control region; FACS, fluorescence-activated cell sorting; *Fgf23*, fibroblast growth factor 23; GFP, green fluorescent protein; M-Csf, colony stimulating factor 1; micro-CT, microcomputed tomography; Rankl, receptor activator of NF-κB ligand; TRAPase, tartrate-resistant acid phosphatase; WT, wild-type.

skeletons (6, 7). DMP1-caPTHR1 mice also exhibit high bone resorption, as evidenced by elevated resorption markers in the blood and urine, high number of osteoclasts in bone, and elevated cortical porosity. Bones from DMP1-caPTHR1 mice display an increased receptor activator of NF-κB ligand (*Rankl*)/*Opg* ratio and elevated macrophage colony-stimulating factor (*M-Csf*) expression. The elevated bone formation and increased bone mass in DMP1-caPTHR1 mice are abolished by overexpressing *Sost* in osteocytes, demonstrating that the increase in osteoblasts is due to reduced sclerostin expression unleashing Wnt signaling (6, 7). On the other hand, increased osteoclast numbers and resorption are not eliminated by *Sost* overexpression. Taken together, these findings demonstrate that PTH receptor signaling in osteocytes regulates bone formation and resorption by distinct mechanisms.

The pro-osteoclastogenic actions of PTH are long recognized to be associated with upregulation of *Rankl* and downregulation of *Opg*. However, the precise differentiation stage of the PTH target cell that supports osteoclastogenesis remains undefined. Osteocytes express high levels of *Rankl* and *Opg* compared with other osteoblastic cells (8–10) and also express *M-Csf* (11, 12). In addition, deletion of the *Rankl* gene from osteocytes leads to osteopetrosis in mice (9, 10). These pieces of evidence raise the possibility that elevated resorption driven by PTH receptor activation in osteocytes could result from direct regulation of osteoclastogenic genes in these cells. By taking advantage of the genetic model of osteocyte-driven bone resorption induced by PTH receptor signaling (DMP1-caPTHR1 mice), we show in this study that removal of the distal control region (DCR) of the *Rankl* gene regulated by PTH gradually corrects the increased resorption exhibited by DMP1-caPTHR1 mice and blunts the high *Rankl* levels in bone. In addition, PTH upregulated *Rankl* expression in authentic osteocytes, in primary cultures of bone cells containing osteocytes, and in bone organ cultures established from wild-type (WT) mice; however, it fails to do so in cultures established from $DCR^{-/-}$ mice. These data show that PTH receptor signaling in osteocytes enhances resorption by regulating the expression of the *Rankl* gene directly in osteocytes.

Materials and Methods

Generation of experimental mice

Experimental animals were generated by a 2-step breeding strategy using transgenic mice expressing a constitutively active PTHR1 in osteocytes under the control of the 8-kb fragment of the promoter of the dentin matrix protein 1 gene (DMP1-caPTHR1) (6) and knock-in mice lacking the distant transcriptional enhancer region in the *Rankl* gene ($DCR^{-/-}$) (13). Heterozygous DMP1-caPTHR1 mice were crossed with $DCR^{-/+}$ mice, and the resulting DMP1-caPTHR1;$DCR^{-/+}$ mice were subsequently crossed with $DCR^{-/+}$ mice. Littermates of the 4 generated genotypes were used for the experiments: WT, DMP1-caPTHR1, $DCR^{-/-}$, and compound DMP1-caPTHR1; $DCR^{-/-}$ mice. All mice were born at the expected Mendelian frequency, were fertile, and exhibited normal size and weight. Cohorts of male and female mice composed of 9 to 16 mice per genotype and gender were used. Mice expressing green fluorescent protein (GFP) in osteocytes (DMP1-GFP) were provided by Dr David W. Rowe and were maintained as homozygous (14). Mice were fed a regular diet (Harlan/Teklad), had ad libitum water, and were maintained on a 12-hour light, 12- hour dark cycle (7). All animal protocols were approved by the Institutional Animal Care and Use Committee at Indiana University School of Medicine.

Quantification of bone turnover markers

Blood was collected monthly by facial vein bleeding into heparinized tubes, and plasma was separated from blood cells by centrifugation at 1500*g* for 10 minutes. C-telopeptide fragments of type I collagen (CTX) were measured using an ELISA (Ratlaps EIA; Immunodiagnostic Systems). Alkaline phosphatase was measured using the AMP buffer (Randox AP 3802) method on a Randox Daytona analyzer (Randox Laboratories Limited) (7).

BMD and microcomputed tomography measurements

Total, femoral, and spine BMD was determined by dual-energy x-ray absorptiometry using a PIXImus II densitometer (GE Medical Systems, Lunar Division), as previously described (6). Mice were anesthetized via inhalation of 2.5% isoflurane (Iso-Flo; Abbott laboratories) mixed with O_2 (1.5 L/min). For microcomputed tomography (micro-CT) analysis, bones were dissected, cleaned of soft tissue, stored in 70% ethanol, and scanned at 6-μm resolution (Skyscan 1172; SkyScan), as previously described (6, 7).

Bone formation rate and tartrate-resistant acid phosphatase staining

Mice were injected with calcein and alizarin red to allow for dynamic histomorphometric measurements, as previously published (7). Femora were fixed in neutral buffer formalin and cut at the midshaft. The distal half of the femur was embedded in methyl metacrylate, and unstained sections were analyzed using the OsteoMeasure high-resolution digital video system (OsteoMetrics, Inc) attached to an Olympus BX51TRF microscope (Olympus America Inc). Only measurements on the endocortical surface were done because by 5 month of age, the action of PTH receptor signaling on the periosteal surface had subsided and the fluorochrome labels on cancellous bone are very intricate, precluding accurate measurement of the bone formation rate (BFR). The proximal half of the femur was decalcified, embedded in paraffin, and sections were stained for tartrate-resistant acid phosphatase (TRAPase) and counterstained with toluidine blue to visualize osteoclasts, as previously described (15). Sections were viewed on a Leitz DMRXE microscope (Leica Mikroskopie

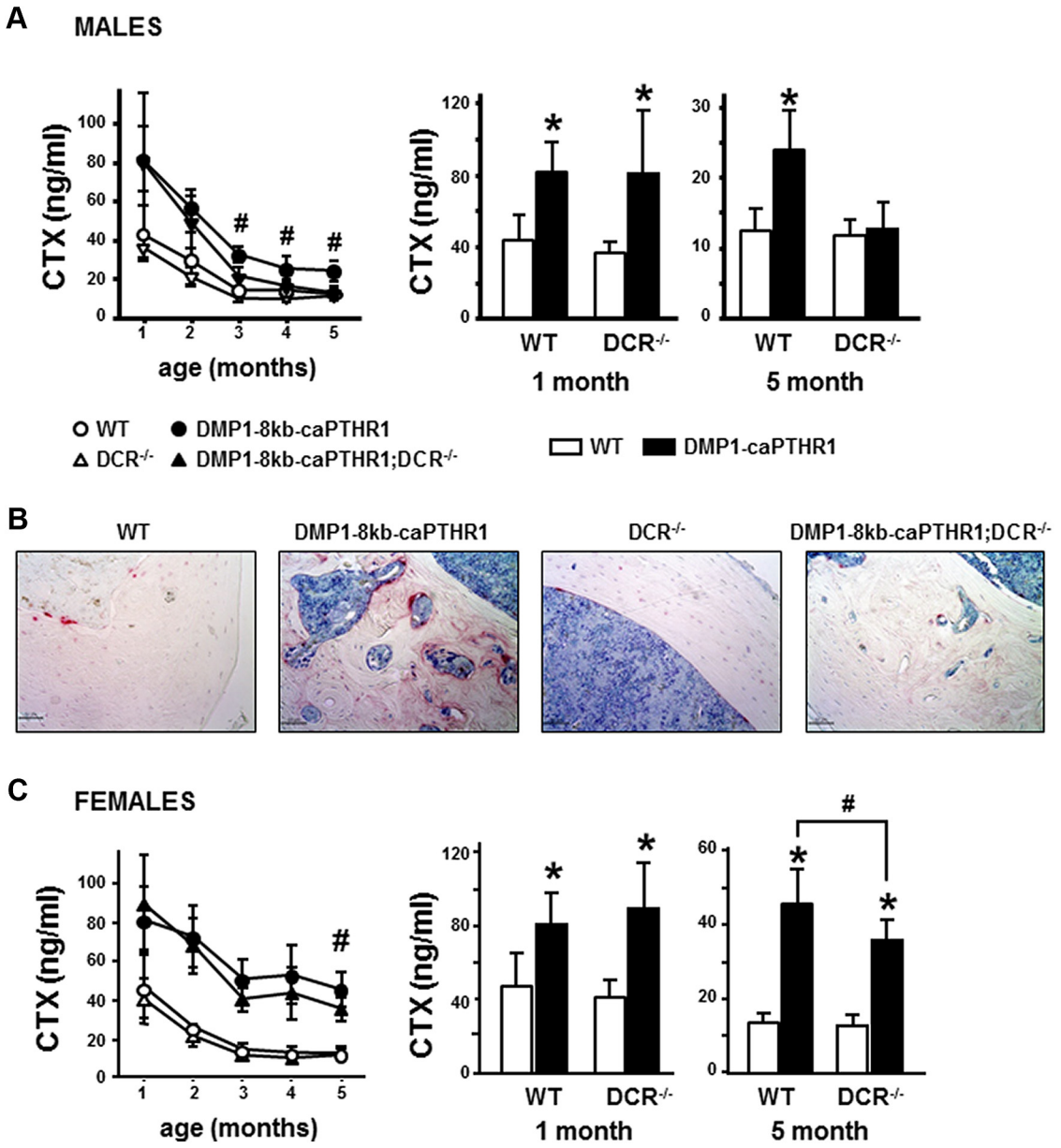

Figure 1. Deletion of the DCR progressively corrects the high resorption induced by PTH receptor signaling in osteocytes in male and female mice. A, Longitudinal analysis of CTX for the male cohort from 1 to 5 months. Symbols represent the means ± SD of 7 to 16 mice per group. #, $P < .05$ for DMP1-caPTHR1 vs DMP1-caPTHR1;DCR$^{-/-}$ CTX levels at 1 and 5 months. Bars represent means ± SD of 7 to 16 mice per group. *, $P < .05$ DMP1-caPTHR1 or DMP1-caPTHR1;DCR$^{-/-}$ vs WT and DCR$^{-/-}$, respectively, by two-way ANOVA. B, Representative images of cross-sections of the femoral midshaft of 5-month-old males stained for TRAPase/toluidine blue. Bars indicate 50 μm. C, Longitudinal analysis of CTX for the female cohort from 1 to 5 months. Symbols represent the means ± SD of 7 to 16 mice per group. #, $P < .05$ DMP1-caPTHR1 vs DMP1-caPTHR1;DCR$^{-/-}$ CTX levels at 1 and 5 months. Bars represent means ± SD of 7 to 16 mice per group. *, $P < .05$ DMP1-caPTHR1 or DMP1-caPTHR1;DCR$^{-/-}$ vs WT and DCR$^{-/-}$, respectively; #, $P < .05$ for conditions connected by the lines, by two-way ANOVA.

und System GmbH). Images were captured using a SPOT digital camera (Diagnostic Instruments, Inc).

Ex vivo bone organ culture and in vitro cell culture

Calvarial bones, femur and tibia were harvested from 5-month old DCR$^{-/-}$ mice and littermate WT controls, maintained in α-MEM containing 10% fetal bovine serum for 24 hours. For osteocyte-enriched bone preparations, tibias were harvested from 5-month-old mice, bone marrow cells were flushed out, and bones were subjected to serial digestions with collagenase and EDTA, as previously published (16). *Sost* expression was 1.5- and 2.4-fold higher in digested WT and DCR$^{-/-}$ bones, respectively, demonstrating osteocyte enrichment. Bones were treated with PTH (100nM) or vehicle for 4 hours, and mRNA was then isolated. Calvarial cells obtained from 1-month-old C57BL/6 mice were cultured to reach confluence, and then medium with ascorbic acid (50 μg/mL) was added for 5 to 6 days, changing half of the medium every 2 to 3 days, as previously described (2). Cells were then treated with PTH (100nM), dibutyryl cAMP (DBA; 1mM) or vehicle for 4 hours.

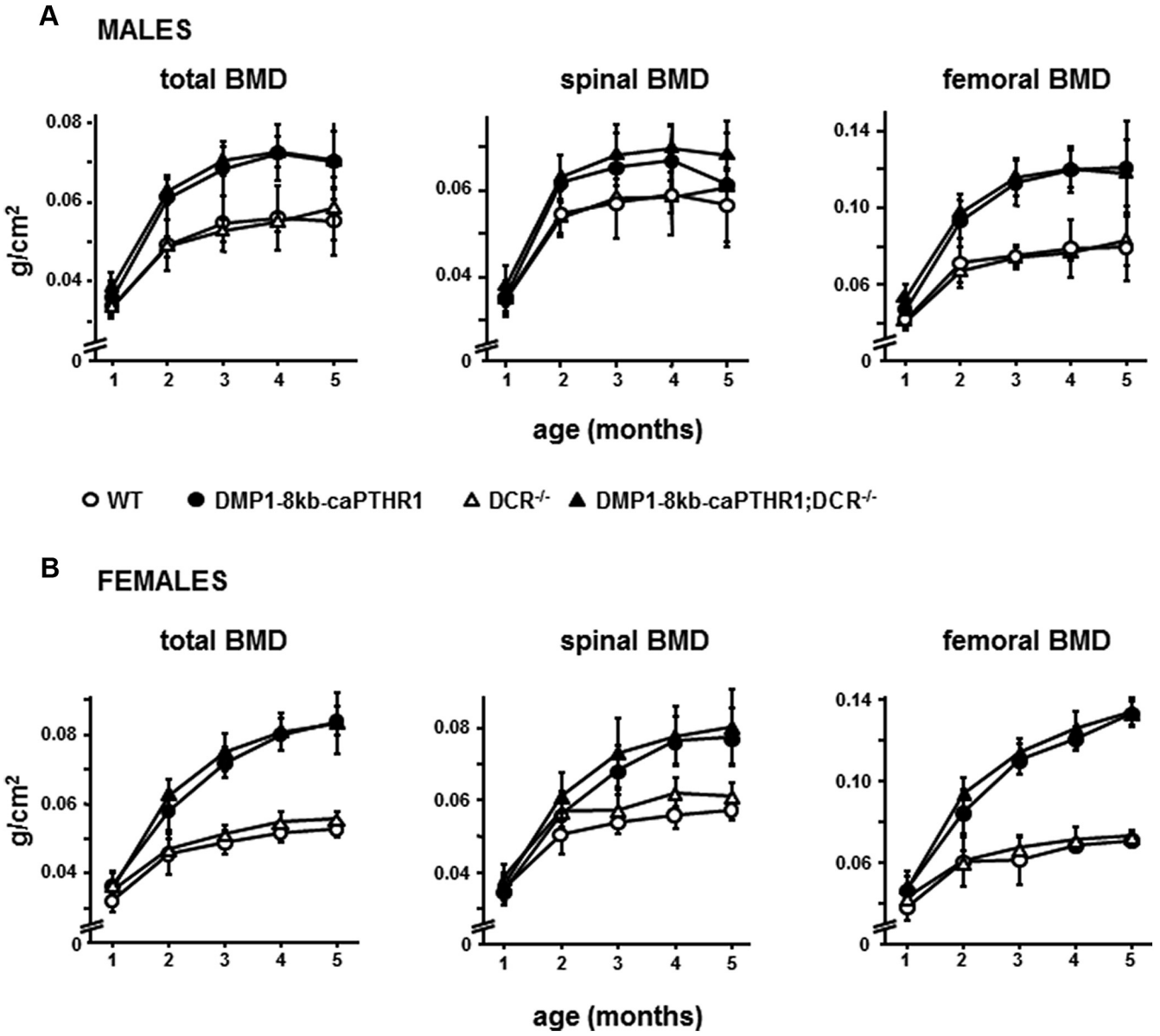

Figure 2. Removal of the DCR does not affect the increase in BMD exhibited by DMP1-caPTHR1 mice. Longitudinal analysis of total, spinal, and femoral BMD in both males (A) and females (B) at 1-month intervals up to 5 months of age. Symbols are means ± SD (n = 7–19 mice per group). No significant differences were detected among phenotypes.

Osteoblasts and osteocytes were isolated from calvarial bones of 9- to 11-day-old DMP1-GFP mice in which osteocytes are labeled with GFP, as previously published (6, 14). Calvarial bones were subjected to 9 sequential 20-minute digestions with a mixture of trypsin/EDTA/collagenase P (17). The first digestion was discarded, and cells from all other digestions were pulled and immediately subjected to fluorescence-activated cell sorting (FACS), as previously reported (6, 18). GFP-positive (osteocytes) and GFP-negative (osteoblasts) cells were cultured separately on plates coated with collagen I as described earlier (19, 20) for 48 hours and treated with PTH (100nM) or vehicle for 4 hours.

Gene expression analysis by quantitative PCR

Calvariae from 1- or 5-month-old mice were cleaned and frozen immediately in liquid nitrogen and stored at −80°C until RNA isolation. Cultured bones or cells were rinsed with PBS, and RNA was immediately isolated. Total RNA was purified using Trizol reagent (Invitrogen) according to the manufacturer's instructions. Gene expression was analyzed by quantitative PCR as previously described using primer probe sets from Applied Biosystems or from Roche Applied Science (6, 7). Relative mRNA expression levels were normalized to the housekeeping genes ribosomal protein S2 (*ChoB*) or glyceraldehyde-3-phosphate dehydrogenase (*Gapdh*) using the cycle threshold (ΔCt) method.

Statistical analysis

Data were analyzed using SigmaStat (SPSS Science). Differences between group means were evaluated using two-way ANOVA, followed by pairwise multiple comparisons using Student-Newman-Keuls method. All values are reported as the mean ± SD.

Results

Deletion of the DCR gradually corrects high resorption and remodeling driven by PTH receptor signaling in osteocytes

To investigate whether direct regulation of the *Rankl* gene by PTH in osteocytes is required to stimulate bone resorption, we examined resorption in DMP1-caPTHR1 mice crossed with knock-in mice lacking the DCR of the *Rankl* gene regulated by PTH. Longitudinal analysis of circulating CTX in male mice showed the expected high resorption in growing mice of all genotypes that progressively decreased to plateau at 3 to 5 months of age (Figure 1A). Resorption was significantly higher (approximately 100%) in DMP1-caPTHR1 mice and nonsignificantly lower (between 15% and 30%) in $DCR^{-/-}$ mice vs WT littermates across all ages. CTX in compound DMP1-caPTHR1;$DCR^{-/-}$ mice was similar to DMP1-caPTHR1 mice at 1 and 2 months of age, but deletion of the DCR gradually corrected the increased resorption exhibited by DMP1-caPTHR1 mice. By 3 months of age, CTX in compound mice was significantly lower compared with DMP1-caPTHR1 mice (and 50% higher than WT), and by 5 months, it was undistinguishable from WT mice. Although accurate measurements of osteoclast numbers for DMP1-caPTHR1 mice at this age are not possible, TRAPase staining of cross-sections at the femoral midshaft show that the abundant TRAPase staining exhibited by DMP1-caPTHR1 bones is decreased in compound mice lacking the DCR (Figure 1B).

Similar results were found in the longitudinal analysis of CTX for female mice. Resorption was high in the first 2 months for all genotypes (Figure 1C). As found for male mice, resorption in DMP1-caPTHR1 female mice was about 70% to 100% higher compared with WT littermates and showed a nonsignificant decrease (7%–13%) in $DCR^{-/-}$ mice compared with WT at all ages. DMP1-caPTHR1;$DCR^{-/-}$ female mice had similar CTX levels to DMP1-caPTHR1 mice for the first 2 months, but at 3 months, DMP1-caPTHR1;$DCR^{-/-}$ female mice showed a significant decrease in CTX compared with DMP1-caPTHR1 mice. CTX remained significantly lower in compound mice at 4 and 5 months of age, but in contrast to male mice, it never reached WT levels. Thus, in female mice, the absence of DCR reduced but did not completely normalize the high resorption induced by the DMP1-caPTHR1 transgene.

DCR deletion did not affect the high BMD exhibited by male or female DMP1-caPTHR1 mice. Thus, longitudinal BMD analysis revealed no significant changes in total, femoral, or spinal BMD in compound DMP1-caPTHR1; $DCR^{-/-}$ compared with DMP1-caPTHR1 littermate male or female mice (Figure 2, A and B). However, micro-CT analysis of femoral bone revealed decreased bone volume in compound male mice compared with DMP1-caPTHR1 littermates (Tables 1 and 2 and Figure 3A). Both bone volume over tissue volume (BV/TV) in the distal femur and bone area over tissue area (BA/TA) in the femoral midhsaft were lower in DMP-caPTHR1 mice with deleted DCR. Dynamic histomorphometric analysis showed that the decreased bone volume in the compound mice was accompanied by a reduced BFR on the endocortical surface of the femur compared with single DMP1-caPTHR1 transgenic mice (Table 3 and Figure 3B). This effect was due to combined reduction in the numbers of osteoblasts covering bone surfaces mineralizing surface over bone surface (MS/BS) and in the activity of osteoblast teams (mineral apposition rate [MAR]). Moreover, although intracortical bone formation could not be quantified, also due to the convoluted fluorochrome incorporation, deletion of the DCR markedly decreased the amount and intensity of fluorescent labels (Figure 3B).

Consistent with these effects on CTX and BFR, circulating levels of the osteoblast marker alkaline phosphatase were elevated in 5-month-old DMP1-caPTHR1 male mice

Table 1. Micro-CT Analysis of Distal Femur in Male Mice[a]

Genotype	BV/TV, %
WT	27.37 ± 3.05
DMP1-caPTHR1	58.37 ± 10.37[b]
$DCR^{-/-}$	31.01 ± 0.48
DMP1-caPTHR1;$DCR^{-/-}$	46.07 ± 10.86[b,c]

[a] Data from 5-month-old male mice are presented. Bone volume over tissue volume (BV/TV) values are means ± SD of 4 to 10 mice per group.

[b] $P < .05$ DMP1-caPTHR1 or DMP1-caPTHR1;$DCR^{-/-}$ vs WT and $DCR^{-/-}$, respectively.

[c] $P < .05$ DMP1-caPTHR1 vs. DMP1-caPTHR1;$DCR^{-/-}$, by two-way ANOVA.

Table 2. Micro-CT Analysis of Femoral Midshaft in Male Mice[a]

Genotype	BA, mm^2	TA, mm^2	BA/TA, %
WT	0.85 ± 0.06	1.96 ± 0.22	43.34 ± 3.68
DMP1-caPTHR1	2.52 ± 0.28[b]	3.03 ± 0.15[b]	83.29 ± 6.69[b]
$DCR^{-/-}$	0.91 ± 0.06	2.04 ± 0.22	44.88 ± 1.98
DMP1-caPTHR1; $DCR^{-/-}$	2.55 ± 0.63[b]	3.38 ± 0.39[b]	75.04 ± 12.08[b,c]

[a] Data from 5-month-old male mice are presented. Bone area (BA), tissue area (TA), and bone area over tissue area (BA/TA) values are means ± SD of 4 to 10 mice per group.

[b] $P < .05$ DMP1-caPTHR1 or DMP1-caPTHR1;$DCR^{-/-}$ vs WT and $DCR^{-/-}$, respectively.

[c] $P < .05$ DMP1-caPTHR1 vs. DMP1-caPTHR1;$DCR^{-/-}$, by two-way ANOVA.

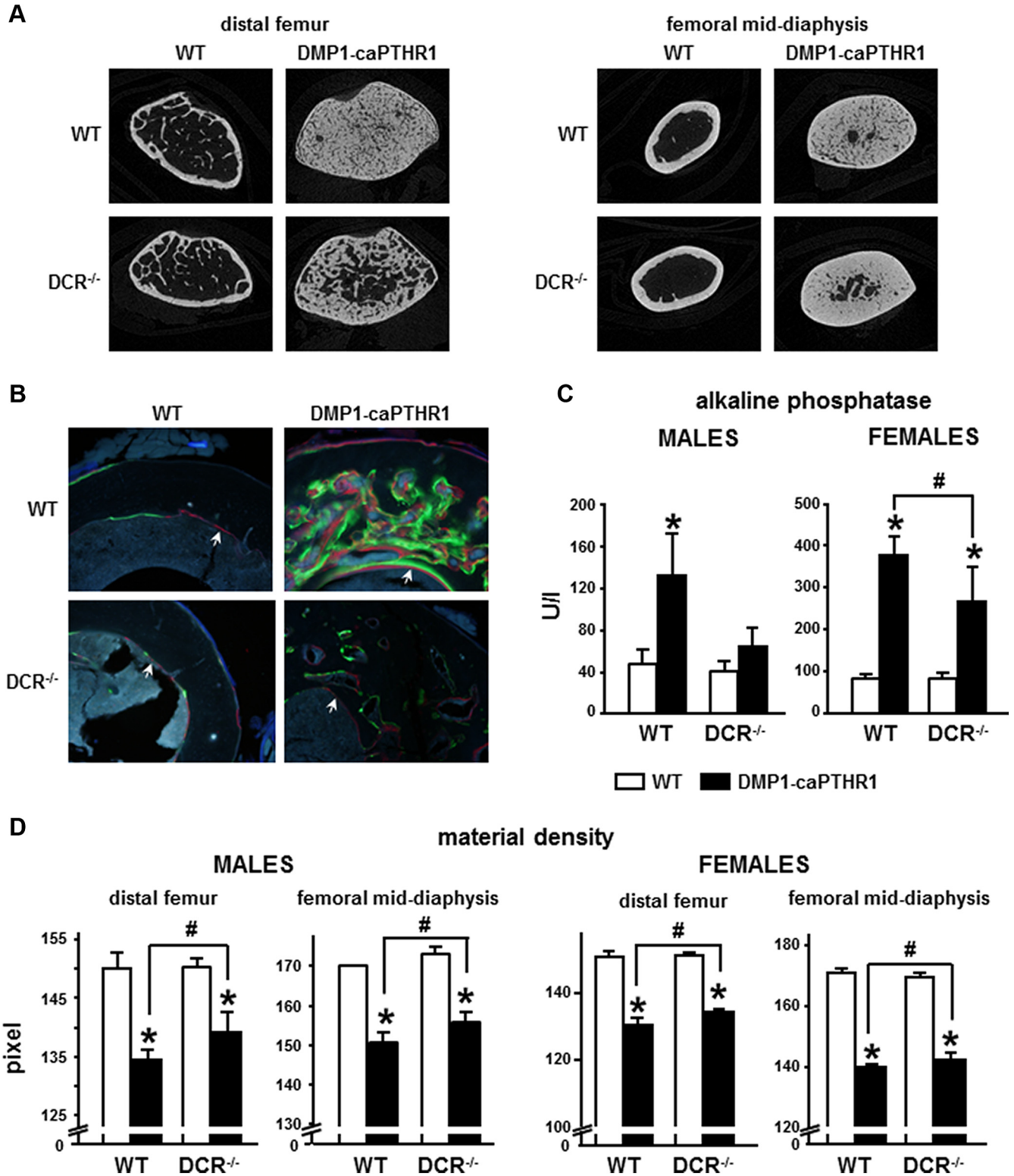

Figure 3. Removal of the DCR blunts the increased bone remodeling induced by PTH receptor activation in osteocytes. A, Representative micro-CT images of distal femur and femoral midshaft of 5-month-old male mice. B, Representative images of unstained cross-sections of the femoral midshaft. Arrows point at the endocortical surface. C, Alkaline phosphatase was measured in plasma from 5-month-old male and female mice for all groups. Bars represent means ± SD of 7 to 11 male mice and 10 to 15 female mice per group. D, Bone material density was determined by micro-CT analysis of femoral bone from 5-month-old mice. Bars represent the means ± SD of 4 to 7 male mice and 4 female mice per group. *, $P < .05$ DMP1-caPTHR1 or DMP1-caPTHR1;DCR$^{-/-}$ vs WT and DCR$^{-/-}$, respectively; #, $P < .05$ for conditions connected by the lines, by two-way ANOVA.

Table 3. Dynamic Histomorphometric Analysis of Endocortical (Ec.) Bone at the Femoral Midshaft in Male Mice[a]

Genotype	Ec. MAR, μm/d	Ec. MS/BS, %	Ec. BFR, $\mu m^3/\mu m^2$/day
WT	0.75 ± 0.28	57.89 ± 12.52	0.44 ± 0.22
DMP1-caPTHR1	1.03 ± 0.25[b]	53.62 ± 10.77	0.57 ± 0.25
$DCR^{-/-}$	0.68 ± 0.26	48.34 ± 7.56	0.33 ± 0.16
DMP1-caPTHR1; $DCR^{-/-}$	0.52 ± 0.21[c]	37.95 ± 7.75[b,c]	0.23 ± 0.10[c]

[a] Data from 5-month-old male mice are presented. Mineral apposition rate (MAR), mineralizing surface over bone surface (MS/BS), and bone formation rate (BFR) values are means ± SD of 4 to 10 mice per group.

[b] $P < .05$ DMP1-caPTHR1 or DMP1-caPTHR1;$DCR^{-/-}$ vs WT and $DCR^{-/-}$, respectively.

[c] $P < .05$ DMP1-caPTHR1 vs. DMP1-caPTHR1;$DCR^{-/-}$, by two-way ANOVA.

and were reduced to WT levels in compound DMP1-caPTHR1;$DCR^{-/-}$ male mice (Figure 3C). A reduction in alkaline phosphatase was also found in female mice, although, similar to CTX levels, alkaline phosphatase levels in compound female mice did not reach WT values (Figure 3C). In addition, DMP1-caPTHR1 bones exhibited lower material density, an index of tissue mineralization that typically is reduced in conditions of high bone remodeling, and this effect was partially corrected in DMP1-caPTHR1 male mice lacking the DCR (Figure 3D). Consistent with the findings for CTX and alkaline phosphatase, the decrease in bone material density exhibited by DMP1-caPTHR1 mice was also prevented to a lesser extent in female than in male mice. Furthermore, micro-CT analysis demonstrate that deletion of the DCR in DMP1-caPTHR1 female mice does not reduce bone volume in either the distal femur or the femoral midshaft (Tables 4 and 5), confirming that the effect of the DCR deletion is weaker in females. Indeed, bone volume at both sites is increased in female compound mice, suggesting that a mild reduction in resorption induced by the DCR deletion is not sufficient

Table 4. Micro-CT Analysis of Distal Femur in Female Mice[a]

Genotype	BV/TV, %
WT	32.37 ± 0.89
DMP1-caPTHR1	89.26 ± 0.79[b]
$DCR^{-/-}$	35.64 ± 1.72
DMP1-caPTHR1;$DCR^{-/-}$	92.49 ± 0.36[b,c]

[a] Data from 5-month-old female mice are presented. Values are means ± SD of 4 mice per group.

[b] $P < .05$ DMP1-caPTHR1 or DMP1-caPTHR1;$DCR^{-/-}$ vs WT and $DCR^{-/-}$, respectively.

[c] $P < .05$ DMP1-caPTHR1 vs. DMP1-caPTHR1;$DCR^{-/-}$, by two-way ANOVA.

Table 5. Micro-CT Analysis of Femoral Midshaft in Female Mice[a]

Genotype	BA, mm^2	TA, mm^2	BA/TA, %
WT	0.81 ± 0.04	1.80 ± 0.06	45.17 ± 1.28
DMP1-caPTHR1	3.52 ± 0.17[b]	3.51 ± 0.19[b]	92.21 ± 0.98[b]
$DCR^{-/-}$	0.93 ± 0.06	1.87 ± 0.08	49.72 ± 1.62
DMP1-caPTHR1; $DCR^{-/-}$	3.59 ± 0.19[b]	3.82 ± 0.19[b]	94.03 ± 0.64[b,c]

[a] Data from 5-month-old female mice are presented. Bone area (BA), tissue area (TA), and bone area over tissue area (BA/TA) values are means ± SD of 4 mice per group.

[b] $P < .05$ DMP1-caPTHR1 or DMP1-caPTHR1;$DCR^{-/-}$ vs WT and $DCR^{-/-}$, respectively.

[c] $P < .05$ DMP1-caPTHR1 vs. DMP1-caPTHR1;$DCR^{-/-}$, by two-way ANOVA.

to inhibit bone formation coupled to resorption, and bone is preserved.

PTH receptor signaling upregulates *Rankl* expression in osteocytes in vivo, ex vivo, and in vitro

The increased resorption exhibited by DMP1-caPTHR1 male mice was accompanied by high *Rankl* mRNA in bone at 1 and 5 months of age (Figure 4A). In compound DMP1-caPTHR1;$DCR^{-/-}$ mice, *Rankl* expression closely matched the described effects on bone resorption. Thus, *Rankl* expression levels were similar to DMP1-caPTHR1 mice at 1 month of age and reduced to WT levels at 5 months. A similar pattern of expression was observed for *M-Csf* (Figure 4B), a survival factor for osteoclast progenitors and mature osteoclasts previously shown to be upregulated by RANKL in cultured RAW 264.7 macrophage cells (21). In addition, the increased expression in bone of TRAPase and cathepsin K, genes expressed in osteoclasts, exhibited by DMP1-caPTHR1 mice was decreased to WT levels in compound DMP1-caPTHR1; $DCR^{-/-}$ male mice (Figure 4C). Similar regulation of *Rankl, M-Csf, Trapase*, and cathepsin K was found in bones from 5-month-old female mice of the 4 genotypes (Figure 4D). These results demonstrate that PTH receptor signaling in osteocytes regulates *Rankl*, as well as *M-Csf* and osteoclastic genes, through the DCR in vivo.

Deletion of the DCR also blunted the increase in *Rankl* expression induced by PTH ex vivo (Figure 5, A and B). Thus, PTH increased *Rankl* and decreased *Sost* and *Opg* expression in calvaria organ cultures established from WT mice. In contrast, the upregulation of the *Rankl* gene was eliminated in bones from $DCR^{-/-}$ mice, whereas *Sost* and *Opg* expression was regulated by PTH to the same extent in $DCR^{-/-}$ and WT bones. Similar regulation of *Rankl* expression by PTH in WT but not in $DCR^{-/-}$ mice was

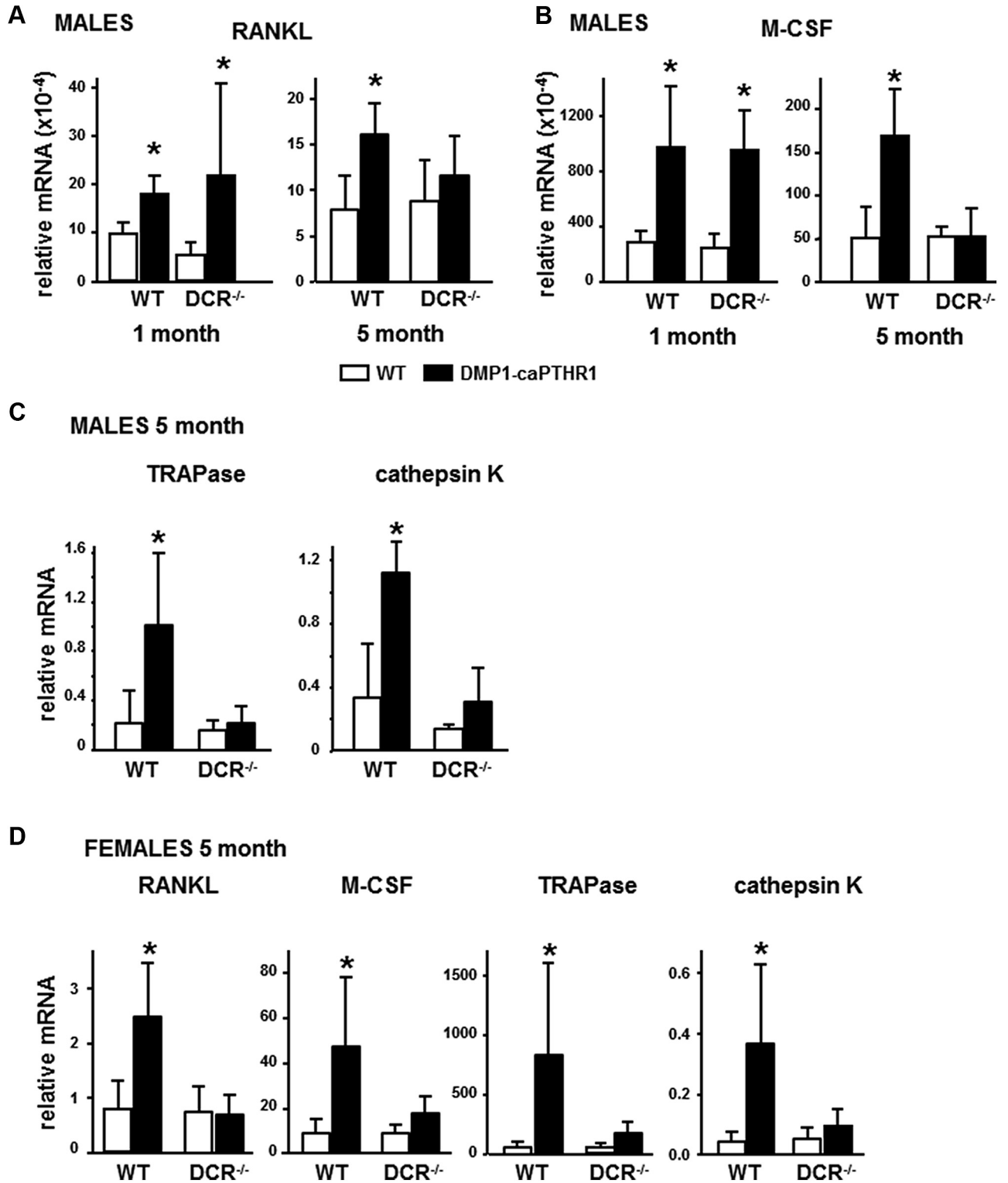

Figure 4. Deletion of the DCR corrects the elevated expression of *Rankl* and *M-Csf* in adult, but not in young, DMP1-caPTHR1 mice. A–C, Quantitative PCR analysis of mRNA transcripts in calvariae from 1- and 5-month-old male mice. Bars represent means ± SD of 3 to 5 mice per group. D, Gene expression in calvaria from 5-month-old female mice. Bars represent means ± SD of 5 mice per group. Results are expressed relative to the housekeeping gene ribosomal protein S2 (*ChoB*). *, $P < .05$ DMP1-caPTHR1 or DMP1-caPTHR1;$DCR^{-/-}$ vs WT and $DCR^{-/-}$, respectively, by two-way ANOVA.

observed in organ cultures of femur or tibia (Figure 5B). Furthermore, PTH increased *Rankl* expression in organ cultures established from tibial bones enriched in osteocytes from WT but not from $DCR^{-/-}$ mice, demonstrating that PTH upregulates *Rankl* expression in osteocytes ex vivo through the DCR.

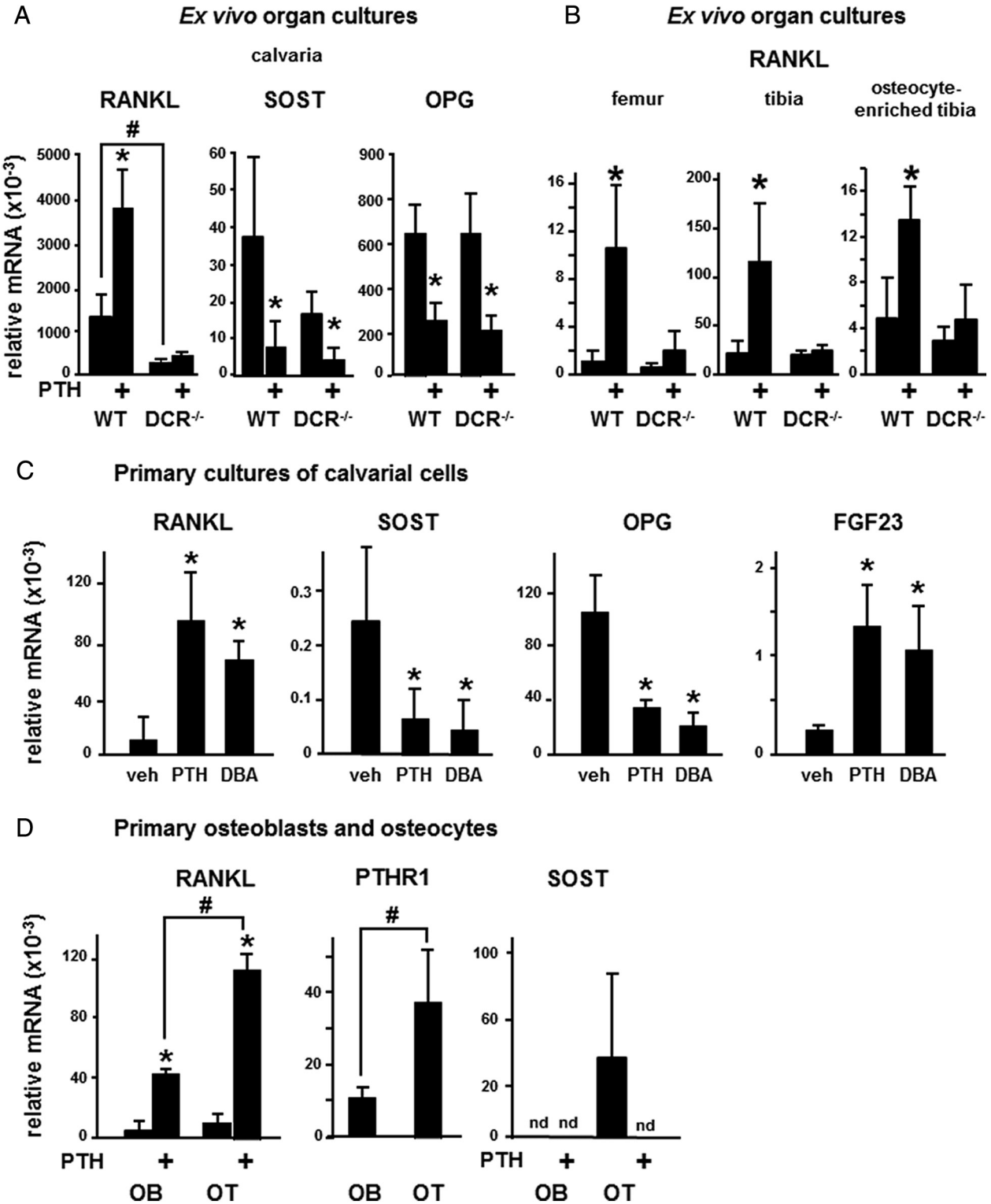

Figure 5. PTH receptor signaling modulates *Rankl* expression in osteocytes in vitro and ex vivo through direct regulation of the *Rankl* gene. The expression of the indicated genes was measured by quantitative PCR. Results are expressed relative to *Gapdh*. A and B, Ex vivo bone organ cultures were cultured overnight and treated with vehicle or PTH for 4 hours. Bars represent mean ± SD of 3 to 5 mice per genotype. *, $P < .05$ DMP1-caPTHR1 or DMP1-caPTHR1;$DCR^{-/-}$ vs WT and $DCR^{-/-}$, respectively; #, $P < .05$ for conditions connected by the lines, by two-way ANOVA. C, Primary cultures of calvaria cells obtained from newborn C57BL/6 mice were treated with vehicle (veh), PTH, or DBA for 4 hours. Bars represent mean ± SD of 5 independent wells per treatment. *, $P < .05$ vs vehicle-treated cultures, by one-way ANOVA. D, Primary osteoblasts (OB) and osteocytes (OT) were isolated by FACS, and the expression of the indicated genes was quantified immediately after sorting. Bars represent mean ± SD of 2 independent wells and duplicate measurements per treatment. *, $P < .05$ PTH vs vehicle-treated cultures by two-way ANOVA; #, $P < .05$ for OT vs OB, by two-way ANOVA (for *Rankl*) or *t* test (for *Pthr1*).

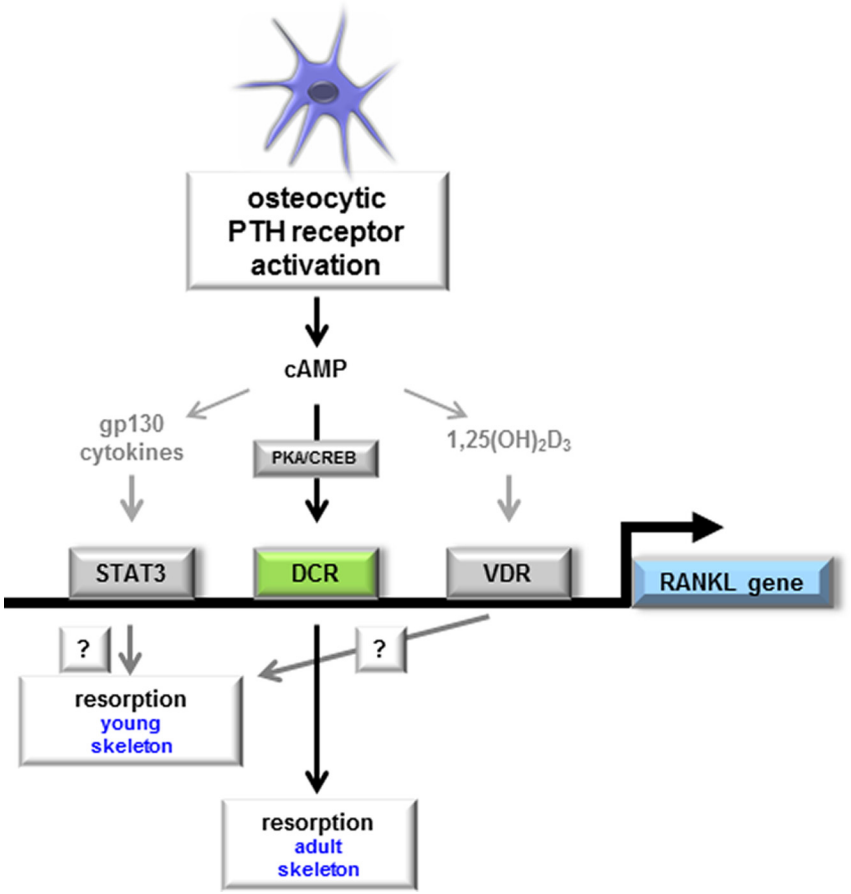

Figure 6. Osteocytic PTH receptor-driven resorption is controlled by the DCR of the *Rankl* gene in the mature skeleton. PTHR1 signaling through cAMP acts directly on the DCR to control *Rankl* expression and resorption in the mature murine skeleton. Stimulation of *Rankl* expression and resorption in the growing skeleton might result from increased gp130 cytokine signaling through signal transducer and activator of transcription 3 (STAT3) response elements or from increased 1,25-dihydroxyvitamin D_3 ($1,25(OH)_2D_3$) mediated by the vitamin D_3 receptor (VDR), or both. PKA, protein kinase A; CREB, cAMP response element-binding protein.

PTH also increased *Rankl* expression in differentiating primary cultures of mouse calvarial cells (Figure 5C). A similar increase was induced by addition of the stable analog of cAMP, DBA. We previously demonstrated that these cultures contain osteocytes, as evidenced by a time-dependent increase in *Sost* transcripts and the presence of sclerostin-positive cells (2). Consistent with these previous findings, *Sost* mRNA was readily detectable after 6 days of culture, and addition of PTH or DBA for 4 hours markedly decreased *Sost* expression. PTH and DBA also decreased expression of *Opg* and increased the expression of *Fgf23*, genes known to be expressed in both osteocytes and osteoblasts.

To discern directly between effects of the hormone on osteoblasts vs osteocytes, authentic cells isolated from calvarial bones of DMP1-GFP mice by controlled enzymatic digestions followed by FACS were maintained in culture and treated with PTH (Figure 5D). Osteocytes (GFP-positive cells) expressed approximately double the amount of *RANKL* transcripts than osteoblasts (GFP-negative cells) (1.8- ± 1.2-fold). PTH stimulated *Rankl* expression in both osteoblasts and osteocytes, although the degree of stimulation was higher in osteocytes than in osteoblasts. Thus, PTH increased *Rankl* expression by 8.88- ± 1.2-fold in osteoblasts and by 12.2- ± 1.9-fold in osteocytes. This difference could be explained potentially by the fact that osteocytes expressed 3.4- ± 0.78-fold more *Pthr1* than osteoblasts. As expected, only osteocytes exhibit transcripts for *Sost*, and PTH eliminated *Sost* expression.

Discussion

It has long been recognized that PTH increases osteoclast production and resorption by upregulating the *Rankl* gene in cells of the osteoblastic lineage. However, the precise differentiation stage of the PTH target cell has been undefined. Recent evidence demonstrates that PTH regulates osteocytic gene expression (1), that osteocytes are an important source of RANKL (22), and that deletion of the PTH receptor from osteocytes decreases *Rankl* expression (23). The findings of the current study demonstrate that resorption induced by PTH receptor signaling in skeletally mature mice requires direct regulation of the *Rankl* gene in osteocytes mediated by the DCR of the gene (Figure 6). Furthermore, we show that PTH regulated *Rankl* expression in osteocyte-containing primary cultures of calvarial cells, in isolated murine osteocytes, and in ex vivo bone organ cultures in a DCR-dependent manner.

In contrast to skeletally mature mice, neither CTX nor *Rankl* transcripts were affected by deletion of the DCR in 1- to 2-month-old mice, indicating that resorption and *Rankl* expression in the growing skeleton of DMP1-caPTHR1 mice are regulated by other factors that do not require the DCR. Osteocyte-derived gp130 cytokines, such as IL-6, IL-11, or oncostatin M could be involved in the stimulation of *Rankl*, because they are expressed by osteocytes and PTH has been shown to stimulate at least IL-6 and IL-11 expression in osteoblastic cells (24–28). In addition, PTH upregulates the expression

of the common signal transducer gp130 in cells of the stromal osteoblastic lineage (27, 29). This evidence raises the possibility that elevated expression of ligands or receptors of this family of cytokines could mediate the increase in *Rankl* expression. In addition, compared with littermate controls, DMP1-caPTHR1 mice exhibit higher circulating levels of 1,25-dihydroxyvitamin D_3 (4, 6), another recognized stimulator of *Rankl* gene transcription.

Most of the circulating products of collagen degradation (CTX) in growing mice (like our 1-month-old mice) are expected to derive from osteoclast activity in cortical bone, the so-called resorptive modeling (30). In contrast, CTX in adult mice (like our 5-month-old mice) probably represent osteoclast activity involved in bone remodeling, to which cancellous bone is a major contributor. The basal phenotype of $DCR^{-/-}$ mice is manifested in adult animals, which exhibit reduced bone remodeling and a modest increase in bone mass confined to the cancellous bone compartment (31). Together with this earlier evidence, our findings showing an age-dependent effect of the DCR deletion on DMP1-caPTHR1 mice suggest that PTH receptor signaling in osteocytes drives resorptive modeling in the growing skeleton mainly through DCR-independent stimulators of *Rankl* expression, such as IL-6–type cytokines, whereas it stimulates resorption in cancellous bone in the adult skeleton via DCR-dependent mechanisms. Future studies are required to identify the DCR-independent mechanisms and bone compartments involved in resorption driven by PTH receptor signaling in the growing skeleton.

Remarkably, in contrast with our findings showing that *Rankl* is equally stimulated in 1-month-old DMP1-caPTHR1 mice regardless of whether DCR is deleted or not, earlier studies showed that endogenous elevation of PTH induced by calcium deficiency does not increase *Rankl* expression in growing mice lacking the DCR (32). The apparent discrepancy could be explained by the different ways of activating PTH receptor signaling. In the paper by O'Brien and colleagues (32), endogenous PTH is elevated systemically, thus affecting all PTH-responsive cells, whereas in the current study, the PTH receptor is activated only in osteocytes. Taken together, these findings suggest that PTH actions in cells other than osteocytes are responsible for the *Rankl* increase with systemic elevation of PTH in growing mice. In contrast, similar to our study, *Rankl* expression induced by endogenous PTH elevation was not increased in adult mice lacking the DCR, suggesting that osteocytes are the major contributors to *Rankl* regulation by PTH in the mature skeleton.

We have previously shown that DMP1-caPTHR1 mice exhibit a consistent decrease in material density of about 10% compared with WT littermates (6, 33). This index measured by micro-CT is indicative of tissue mineralization and age of the mineral. Reduced values of bone material density reveal accumulation of undermineralized bone, which could result from an increased bone remodeling rate that does not give enough time for the new bone to fully mineralize or from abnormal mineralization. We have shown that further stimulation of resorption in the DMP1-caPTHR1 mice decreased material density even more. Conversely, treatment of DMP1-caPTHR1 mice with bisphosphonates, which strongly inhibits resorption, increased material density by 7.4% toward values found in WT mice (33). In the current study, we found that deletion of the DCR, which blocks only PTH-induced Rankl-mediated resorption, also increases material density in DMP1-caPTHR1 mice but to a lesser extent, by 3.7%. Taken together, these pieces of evidence suggest that in the DMP1-caPTHR1 mouse model, bone material density is regulated by changes in resorption and that deletion of the DCR decreases the rate of bone remodeling leading to bone with higher levels of mineralization. Nevertheless, decreased material density could result also from defective mineralization, potentially caused by decreased 1,25-dihydroxyvitamin D_3 or phosphate or to increased Fgf23. However, 1,25-dihydroxyvitamin D_3 is actually increased and phosphate is not altered in DMP-caPTHR1 mice, as reported earlier (4, 6). Although young DMP-caPTHR1 mice do exhibit increased *Fgf23* that could have an impact on bone mineralization (4), *Fgf23* was practically undetectable in bones from the 5-month-old mice used in this study, of any genotype and gender. Therefore, we cannot attribute the partial rescue of bone material density observed in compound DMP1-caPTHR1;$DCR^{-/-}$ mice to changes in *Fgf23* expression.

RANKL and M-CSF are 2 major factors that contribute to osteoclast differentiation and maturation. In the present study, we found that *M-Csf* mRNA levels in bone exhibited a similar pattern of expression to *Rankl* transcripts. Deletion of the DCR eliminates the ability of the PTH receptor/cAMP pathway to increase *Rankl* expression. Thus, the fact that at 5 months of age the expression of both *Rankl* and *M-Csf* was reduced in DMP1-caPTHR1; $DCR^{-/-}$ mice compared with single DMP1-caPTHR1 transgenic mice demonstrates that *M-Csf* regulation is secondary to *Rankl* regulation. To our knowledge, this evidence is the first in vivo demonstration of *M-Csf* regulation by RANKL and is consistent with an earlier in vitro study showing that RANKL augmented *M-Csf* production in preosteoclastic cells (21). The regulation of *M-Csf* by RANKL appears counterintuitive, because M-Csf increases the expression of the RANKL receptor RANK in osteoclast precursors (34), suggesting that M-CSF is needed for RANKL signaling. However, deletion of the

DCR reverses only the PTHR1-induced *M-Csf* expression, demonstrating that basal levels of M-Csf are sufficient to induce *Rank* expression and to allow the initial action of PTH-stimulated osteocytic RANKL. RANKL/RANK signaling in turn could induce higher *M-Csf* expression in a positive feedback loop, stimulating osteoclastogenesis. Furthermore, *M-Csf* is expressed not only in osteoclast precursors but also in osteocytes (11, 12) suggesting that RANKL (either membrane-bound or soluble form) could upregulate *M-Csf* gene expression in osteoclast precursors or in osteocytes. Future studies are required to determine the cellular source of *M-Csf* in osteocyte-driven resorption induced by PTH receptor activation.

Despite the marked effects on resorption driven by PTH receptor signaling in osteocytes, deletion of the DCR did not affect BMD. DMP1-caPTHR1 mice exhibit high bone mass with elevated bone resorption and formation (6, 7, 33). Therefore, inhibition of resorption could lead to even higher BMD. However, we found that bone volume is reduced and alkaline phosphatase levels in the circulation are decreased in compound DMP1-caPTHR1;DCR$^{-/-}$ male mice compared with single transgenic DMP1-caPTHR1 mice. Moreover, bone formation on the endocortical surface of the femoral midshaft is also reduced by deletion of the DCR. Thus, the lack of an increase in BMD in the face of reduced resorption is explained by concomitant reduced bone formation. These findings are consistent with our earlier evidence demonstrating that bone formation on the endocortical surface of DMP1-caPTHR1 mice results from a combination of Wnt-dependent increased osteoblast number and resorption-driven osteoblast activity (33).

In contrast to our findings with male mice in which the DCR deletion abolishes completely resorption at 5 month of age, DCR deletion has a weaker effect on resorption in female DMP-caPTHR1 mice. This could be explained by the higher bone remodeling rate exhibited by female compared with male mice (2-fold higher CTX and 3-fold higher alkaline phosphatase). Nevertheless, deletion of the DCR reduces effectively the expression of *Rankl, M-Csf*, and osteoclast markers in females, suggesting that given enough time, compound female mice would exhibit a complete reversal of resorption toward WT levels.

It is important to distinguish our study from that of Leder and colleagues (35) in which daily injections of PTH (1–34) combined with an anti-RANKL antibody increased BMD more than PTH alone in humans. In our study, activation of PTH receptor signaling is confined to osteocytes, and consequently, the expression of *Rankl* is increased (or not in the absence of DCR) solely in osteocytes. Thus, deleting the DCR does not remove the effect of PTH on *Rankl* expressed in other bone cells or the effects of the hormone on other genes such as *Sost* and *Opg*. Furthermore, PTH receptor signaling in the DMP1-caPTHR1 mice is activated in a continuous manner, not in an intermittent mode. These differences might explain the failure of DCR deletion to further increase BMD in DMP1-caPTHR1 mice. An experiment more comparable to the study by Leder and colleagues (35) would be administration of bisphosphonates to DMP1-caPTHR1 mice, which did increase BMD over the anabolic effect of PTH receptor activation in osteocytes as we published earlier (33).

In conclusion, resorption induced by PTH receptor signaling in osteocytes requires direct regulation of the *Rankl* gene in osteocytes. Thus, whereas DCR-independent mechanisms operate in the growing skeleton, DCR-dependent, cAMP-activated mechanisms mediate resorption induced by PTH receptor signaling in the adult skeleton.

Acknowledgments

We thank Dr Keith Condon and Ms Naomie Olivos for technical assistance and Dr Munro Peacock for measurement of alkaline phosphatase.

Address all correspondence and requests for reprints to: Teresita Bellido, PhD, Departments of Anatomy and Cell Biology and Internal Medicine, Endocrinology, Indiana University School of Medicine, 635 Barnhill Drive, MS5045A, Indianapolis, IN 46202. E-mail: tbellido@iupui.edu.

This research was supported by the National Institutes of Health (R01DK076007 and American Recovery and Reinvestment Act supplement S10-RR023710 to T.B.) and the Veterans Administration (Merit Review I01BX002104 to T.B.).

Disclosure Summary: The authors declare that no conflict of interest exists.

References

1. **Bellido T, Saini V, Pajevic PD.** Effects of PTH on osteocyte function. *Bone*. 2013;54:250–257.
2. **Bellido T, Ali AA, Gubrij I, et al.** Chronic elevation of parathyroid hormone in mice reduces expression of sclerostin by osteocytes: a novel mechanism for hormonal control of osteoblastogenesis. *Endocrinology*. 2005;146:4577–4583.
3. **Keller H, Kneissel M.** SOST is a target gene for PTH in bone. *Bone*. 2005;37:148–158.
4. **Rhee Y, Bivi N, Farrow E, et al.** Parathyroid hormone receptor signaling in osteocytes increases the expression of fibroblast growth factor-23 in vitro and in vivo. *Bone*. 2011;49:636–643.
5. **Lavi-Moshayoff V, Wasserman G, Meir T, Silver J, Naveh-Many T.** PTH increases FGF23 gene expression and mediates the high-FGF23 levels of experimental kidney failure: a bone parathyroid feedback loop. *Am J Physiol Renal Physiol*. 2010;299:F882–F889.
6. **O'Brien CA, Plotkin LI, Galli C, et al.** Control of bone mass and

remodeling by PTH receptor signaling in osteocytes. *PLoS One*. 2008;3:e2942.
7. **Rhee Y, Allen MR, Condon K, et al.** PTH receptor signaling in osteocytes governs periosteal bone formation and intracortical remodeling. *J Bone Miner Res*. 2011;26:1035–1046.
8. **Kramer I, Halleux C, Keller H, et al.** Osteocyte Wnt/beta-catenin signaling is required for normal bone homeostasis. *Mol Cell Biol*. 2010;30:3071–3085.
9. **Xiong J, Onal M, Jilka RL, Weinstein RS, Manolagas SC, O'Brien CA.** Matrix-embedded cells control osteoclast formation. *Nat Med*. 2011;17:1235–1241.
10. **Nakashima T, Hayashi M, Fukunaga T, et al.** Evidence for osteocyte regulation of bone homeostasis through RANKL expression. *Nat Med*. 2011;17:1231–1234.
11. **Zhao S, Zhang YK, Harris S, Ahuja SS, Bonewald LF.** MLO-Y4 osteocyte-like cells support osteoclast formation and activation. *J Bone Miner Res*. 2002;17:2068–2079.
12. **Harris SE, MacDougall M, Horn D, et al.** Meox2Cre-mediated disruption of CSF-1 leads to osteopetrosis and osteocyte defects. *Bone*. 2012;50:42–53.
13. **Fu Q, Manolagas SC, O'Brien CA.** Parathyroid hormone controls receptor activator of NF-kappaB ligand gene expression via a distant transcriptional enhancer. *Mol Cell Biol*. 2006;26:6453–6468.
14. **Kalajzic I, Braut A, Guo D, et al.** Dentin matrix protein 1 expression during osteoblastic differentiation, generation of an osteocyte GFP-transgene. *Bone*. 2004;35:74–82.
15. **Erlebacher A, Derynck R.** Increased expression of TGF-beta 2 in osteoblasts results in an osteoporosis-like phenotype. *J Cell Biol*. 1996;132:195–210.
16. **Stern AR, Stern MM, Van Dyke ME, Jähn K, Prideaux M, Bonewald LF.** Isolation and culture of primary osteocytes from the long bones of skeletally mature and aged mice. *Biotechniques*. 2012;52:361–373.
17. **Paic F, Igwe JC, Nori R, et al.** Identification of differentially expressed genes between osteoblasts and osteocytes. *Bone*. 2009;45:682–692.
18. **Bivi N, Condon KW, Allen MR, et al.** Cell autonomous requirement of connexin 43 for osteocyte survival: consequences for endocortical resorption and periosteal bone formation. *J Bone Miner Res*. 2012;27:374–389.
19. **Plotkin LI, Weinstein RS, Parfitt AM, Roberson PK, Manolagas SC, Bellido T.** Prevention of osteocyte and osteoblast apoptosis by bisphosphonates and calcitonin. *J Clin Invest*. 1999;104:1363–1374.
20. **Kato Y, Windle JJ, Koop BA, Mundy GR, Bonewald LF.** Establishment of an osteocyte-like cell line, *MLO-Y4*. *J Bone Miner Res*. 1997;12:2014–2023.
21. **Islam S, Hassan F, Tumurkhuu G, et al.** Receptor activator of nuclear factor-kappa B ligand induces osteoclast formation in RAW 264.7 macrophage cells via augmented production of macrophage-colony-stimulating factor. *Microbiol Immunol*. 2008;52:585–590.
22. **O'Brien CA, Nakashima T, Takayanagi H.** Osteocyte control of osteoclastogenesis. *Bone*. 2013;54:258–263.
23. **Saini V, Marengi DA, Barry KJ, et al.** Parathyroid hormone (PTH)/PTH-related peptide type 1 receptor (PPR) signaling in osteocytes regulates anabolic and catabolic skeletal responses to PTH. *J Biol Chem*. 2013;288:20122–20134.
24. **Sakagami Y, Girasole G, Yu XP, Boswell HS, Manolagas SC.** Stimulation of interleukin-6 production by either calcitonin gene-related peptide or parathyroid hormone in two phenotypically distinct bone marrow-derived murine stromal cell lines. *J Bone Miner Res*. 1993;8:811–816.
25. **Feyen JH, Elford P, Di Padova FE, Trechsel U.** Interleukin-6 is produced by bone and modulated by parathyroid hormone. *J Bone Miner Res*. 1989;4:633–638.
26. **Lin SC, Yamate T, Taguchi Y, et al.** Regulation of the gp80 and gp130 subunits of the IL-6 receptor by sex steroids in the murine bone marrow. *J Clin Invest*. 1997;100:1980–1990.
27. **Romas E, Udagawa N, Zhou H, et al.** The role of gp130-mediated signals in osteoclast development: regulation of interleukin 11 production by osteoblasts and distribution of its receptor in bone marrow cultures. *J Exp Med*. 1996;183:2581–2591.
28. **O'Brien CA.** Control of RANKL gene expression. *Bone*. 2010;46:911–919.
29. **Shin HI, Divieti P, Sims NA, et al.** Gp130-mediated signaling is necessary for normal osteoblastic function in vivo and in vitro. *Endocrinology*. 2004;145:1376–1385.
30. **Allen MR, Burr DB.** Bone modeling and remodeling. In: Burr D, Allen M, eds. *Basic and Applied Bone Biology*. 1st ed. Elsevier; 75–90; 2014.
31. **Galli C, Zella LA, Fretz JA, Fu Q, Pike JW, Weinstein RS, Manolagas SC, O'Brien CA.** Targeted deletion of a distant transcriptional enhancer of the RANKL gene reduces bone remodeling and increases bone mass. *Endocrinology*. 2007;149:146–153.
32. **Onal M, Galli C, Fu Q, Xiong J, Weinstein RS, Manolagas SC, O'Brien CA.** The RANKL distal control region is required for the increase in RANKL expression, but not the bone loss, associated with hyperparathyroidism or lactation in adult mice. *Mol Endocrinol*. 2012;26:341–348.
33. **Rhee Y, Lee EY, Lezcano V, Ronda AC, Condon KW, Allen MR, Plotkin LI, Bellido T.** Resorption controls bone anabolism driven by PTH receptor signaling in osteocytes. *J Biol Chem*. 2013;288:29809–29820.
34. **Bellido T, Plotkin LI, Bruzzaniti A.** 2014 Bone cells. In: Burr D, Allen M, eds. Basic and Applied Bone Biology. First ed. Atlanta: Elsevier; 27–45.
35. **Tsai JN, Uihlein AV, Lee H, et al.** Teriparatide and denosumab, alone or combined, in women with postmenopausal osteoporosis: the DATA study randomised trial. *Lancet*. 2013;382:50–56.